

Modeling of Microdiaphragm Based Pressure Sensor with Application for Gas Turbine Engine Condition Monitoring

¹ Ahmad GHANBARI, ² Ehsan QAREDAGHI

¹ Department of Mechanical Engineering,

School of Engineering-Emerging Technologies, University of Tabriz, Tabriz, Iran

² School of Engineering-Emerging Technologies, University of Tabriz, Tabriz, Iran

E-mail: a-ghanbari@tabrizu.ac.ir, e.qaredaghi@gmail.com

Received: 23 April 2013 /Accepted: 25 August 2013 /Published: 30 September 2013

Abstract: The miniaturization of sensors represents a promising approach for various systems health management. Dynamic pressure measurements have a very good potential to provide GTE diagnostics, maintenance management, and optimized performance, based on pressure variation measurements. In this paper, we will investigate vibrational behavior of piezoelectric microdiaphragm based pressure sensor with application for GTEs condition monitoring. The general formulation based on transverse vibration of circular plates will be introduced and the response of diaphragm under forced excitation will be discussed. The obtained results show that the application of pressure sensor for condition monitoring of GTEs could have major benefits and improve their performance. Copyright © 2013 IFSA.

Keywords: MEMS, Pressure sensor, Piezoelectric, GTEs, Condition monitoring, Transverse vibration, Circular microdiaphragm.

1. Introduction

The miniaturization of sensors represents a promising approach for various systems health management. The main advantages of miniaturized systems include low mass and low power consumption. MEMS based sensor systems will play a significant role in the development of miniature, on-line, in-situ, low cost, health monitoring platforms.

In literature, many condition monitoring applications have been proposed for pressure sensors [1-7]. One application area with major impact is condition monitoring of Gas Turbine Engines (GTEs) [1]. The application of MEMS pressure sensors makes it possible obtaining engine

performance characteristics with high sensitivity and fast response time. Moreover, these devices replace macro-sensors which provide offline condition monitoring.

For these purposes, dynamic behavior characterization of microdiaphragm based pressure sensors could help to optimize the health management system and provide better performance for GTEs. Many researches have been done to characterize dynamic behavior of circular microdiaphragms. Yu et al. have been introduced a mathematical modeling of microdiaphragms under initial tension [13]. Olfatnia et al. theoretically modeled the dynamic behavior of circular microdiaphragms and the influences of pressure loading on the behavior of the diaphragm in different vibration modes [8-10].

In this paper, first we acquire the mathematical formulation of dynamic behavior of circular microdiaphragm including damped condition. Then, a model will be introduced to be applicable to GTEs condition monitoring.

2. Theory

2.1. General Formulation

The sensor is modeled as a clamped circular diaphragm with initial tension and rigidity, as shown in Fig. 1, with radius a , thickness h , Young's modulus E , and Poisson's ratio ν . The non-linear partial differential equation of that diaphragm with a transverse loading per unit area, is governed as equation [14]

$$\rho h \frac{\partial^2 w}{\partial t^2} + D\nabla^4 - T\nabla^2 w = -2\mu \frac{\partial w}{\partial t} + f(r, \theta, t), \quad (1)$$

where ρ is the density, w is the transverse displacement and

$$D = Eh^3 / 12(1-\nu^2), \quad (2)$$

is the flexural rigidity, ∇^2 is the laplacian, and T is the initial tension of the diaphragm per unit length. The boundary conditions are as follow:

$$w(a, \theta, t) = 0, \quad \left. \frac{\partial w(r, \theta, t)}{\partial r} \right|_{r=a} = 0. \quad (3)$$

In the absence of forcing in equation (1), we will search for a modal solution of form

$$w(r, \theta, t) = W(r, \theta) e^{(\alpha+i\omega)t}, \quad (4)$$

where W is the unknown function, α is the term characterizing damped condition, and ω is natural frequency. Substituting (4) into equation (1), we obtain

$$\begin{aligned} & [(\alpha^2 - \omega^2 + 2i\alpha\omega)\rho h + 2\mu(\alpha + i\omega)]W \\ & + D\nabla^4 W - T\nabla^2 W = 0. \end{aligned} \quad (5)$$

Equation (5) can be expressed as

$$(\nabla^2 + \gamma_1^2)(\nabla^2 - \gamma_2^2)W = 0. \quad (6)$$

It is found that

$$\begin{aligned} \gamma_1^2 &= \frac{-T + \sqrt{T^2 - 4D\Gamma}}{2D}, \\ \gamma_2^2 &= \frac{+T + \sqrt{T^2 - 4D\Gamma}}{2D}, \end{aligned} \quad (7)$$

where Γ is as follow:

$$\Gamma = \rho h (\alpha^2 - \omega^2) + 2\mu\alpha + 2i\omega(\mu + \rho h \alpha). \quad (8)$$

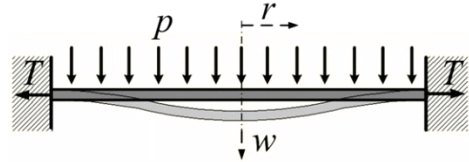


Fig. 1. Illustration of the clamped diaphragm [8].

It can be shown that

$$\alpha = -\frac{\mu}{\rho h}. \quad (9)$$

Expanding the transverse displacement amplitude as

$$W(r, \theta) = R(r)\Theta(\theta), \quad (10)$$

results in equation (11),

$$\begin{aligned} \Theta(\theta) &= A_{1m} \sin m\theta + A_{2m} \cos m\theta \\ R(r) &= B_{1m} J_m(\gamma_{1m} r) + B_{2m} Y_m(\gamma_{1m} r) \\ &+ B_{3m} I_m(\gamma_{2m} r) + B_{4m} K_m(\gamma_{2m} r) \end{aligned} . \quad (11)$$

The solution of equation (11) must be continuous, and therefore m must be an integer. The functions J_m , Y_m , I_m , and K_m are the Bessel functions of the first and second kind, and the modified Bessel functions of the first and second kind, respectively. The coefficients A and B in equation (11) are constants which are determined by the boundary conditions. Both Y_m and K_m are singular at $r = 0$. Therefore, for a plate with a finite displacement at the plate center, the coefficients B_{2m} and B_{4m} are equal to zero. Applying function $R(r)$ into the boundary condition, equation (3) results in the following equation

$$\begin{bmatrix} J_m(\gamma_{1m} a) & I_m(\gamma_{2m} a) \\ J'_m(\gamma_{1m} a) & I'_m(\gamma_{2m} a) \end{bmatrix} \begin{bmatrix} B_{1m} \\ B_{3m} \end{bmatrix} = 0. \quad (12)$$

The prime indicates a derivative with respect to r . For non-trivial solutions of B_{1m} and B_{3m} , the characteristic equation should be equal to zero:

$$\begin{aligned} & J_m(\gamma_{1m} a) J_m(\gamma_{1m} a) \\ & - I_m(\gamma_{2m} a) J'_m(\gamma_{1m} a) = 0. \end{aligned} \quad (13)$$

By determining the roots of equation (13), and replacing them into the rearranged form of equation (7), the natural frequencies are obtained as follows:

$$\omega_{mn}^d = \sqrt{\frac{1}{\rho h} \left(D \gamma_{1mn}^4 + T \gamma_{1mn}^2 \right) - \left(\frac{\mu}{\rho h} \right)^2}, \quad (14)$$

where the superscript d shows the damped natural frequency. Under un-damped condition the natural frequency is as follows [9]:

$$\omega_{mn}^n = \sqrt{\frac{1}{\rho h} \left(D \gamma_{1mn}^4 + T \gamma_{1mn}^2 \right)}. \quad (15)$$

If we assume that,

$$\frac{\mu}{\rho h} = \zeta_{mn} \omega_{mn}^n, \quad (16)$$

we can rewrite equation (14) as follows

$$\omega_{mn}^d = \omega_{mn}^n \sqrt{1 - \zeta_{mn}^2}, \quad (17)$$

Finally, the mode shape is obtained as follows:

$$\begin{aligned} W(r, \theta) &= R(r) \Theta(\theta) \\ R(r) &= J_m(\gamma_{1mn} r) - \frac{J_m(\gamma_{1mn} a)}{I_m(\gamma_{2mn} a)} I_m(\gamma_{2mn} r), \quad (18) \\ \Theta(\theta) &= A_{1m} \sin m\theta + A_{2m} \cos m\theta \end{aligned}$$

A non-dimensional tension parameter k is defined as [11]

$$k = a \sqrt{\frac{T}{D}}, \quad (19)$$

This non-dimensional parameter determines the behavior of the diaphragm. If the internal tension is so high that it dominates the flexural rigidity, the diaphragm behaves as tension dominated membrane. On the other hand, if internal tensions are so low that flexural rigidity is dominated, the diaphragm behaves as flexural rigidity dominated plate.

Fig. 2 shows the natural frequency versus k . As it is obvious from the figure, if k is less than 1 the flexural rigidity is dominated, if k is greater than 20 tension is dominated, and the range between this two values is called transition region, and in this region diaphragm behaves between plate and membrane.

The effect of parameter k is not limited to determination of natural frequency. We can conclude from equation (7):

$$\gamma_{2mn}^2 = \gamma_{1mn}^2 + k. \quad (20)$$

This means that k effects mode shapes through characteristic equation. Fig. 3 shows first vibrational mode of diaphragm respect to different values of k .

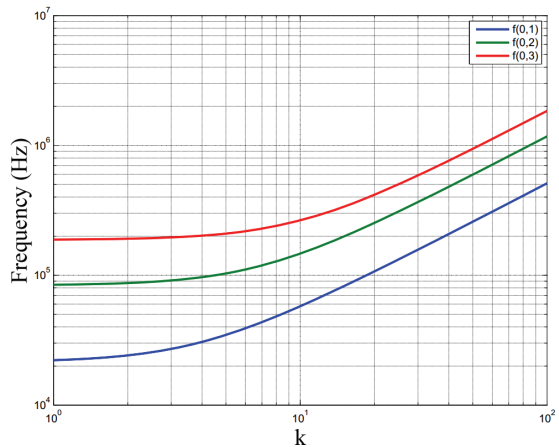


Fig 2. Variations of the first three resonant frequencies with respect to the tension parameter k .

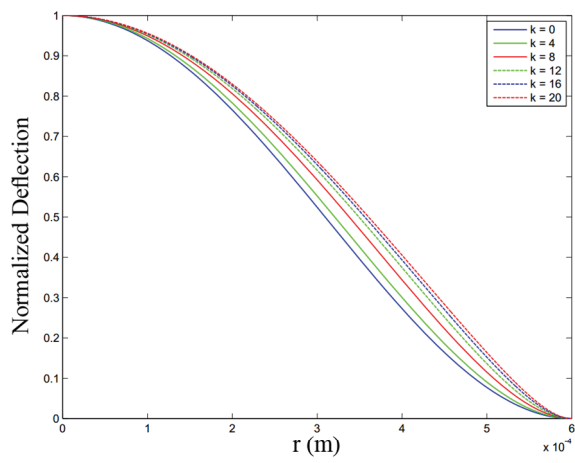


Fig 3. Variation of first mode shape with respect to parameter k .

2.2. Forced Response

To consider the forced response of a damped diaphragm to harmonic excitations loading is assumed to be the form

$$f(r, \theta, t) = p(r, \theta) e^{i\omega t}, \quad (21)$$

where the pressure amplitude $p(r, \theta)$ is assumed to be uniform and denoted by p , and ω is the excitation frequency. The aim is to find the steady state response of the diaphragm when it is excited close to the diaphragms first natural frequency. To that end, to that end, a single-mode approximation is assumed as

$$w(r, \theta, t) \approx W_{01}(r, \theta) \eta_1(t), \quad (22)$$

where η_1 is the modal amplitude and W_{01} is the first mode shape of the linear system. The approximation

for the steady state forced response of the diaphragm can be obtained as

$$w(r, \theta, t) \approx U(r, \theta) e^{i(\omega t - \phi_0)} \\ = \Lambda_{01} W_{01}(r, \theta) e^{i(\omega t - \phi_0)}. \quad (23)$$

It can be shown that vibration amplitude, $U(r, \theta)$, at the center of the diaphragm is as follow [13]:

$$U(0, \theta) = \frac{2\pi pa}{\rho h T} \left[1 - \frac{J_0(\gamma_{101}a)}{I_0(\gamma_{201}a)} \right] \\ \times \left[\frac{1}{\gamma_{101}} J_1(\gamma_{101}a) - \frac{J_0(\gamma_{101}a)}{\gamma_{201} I_0(\gamma_{201}a)} I_1(\gamma_{201}a) \right]. \quad (24)$$

$$\omega_1 \sqrt{\left[1 - \left(\frac{\omega}{\omega_{01}} \right)^2 \right]^2 + 4\zeta_{01}^2 \left(\frac{\omega}{\omega_{01}} \right)^2}$$

3. Validation

For validation of our general formulation of damped vibration of diaphragm, we used the experimental results obtained by Olfatnia et al. [9]. Fig. 4 shows the configuration of diaphragm used by Olfatnia et al. for experimental purposes. This figure shows that multi-morph diaphragm consist of 5 layers.

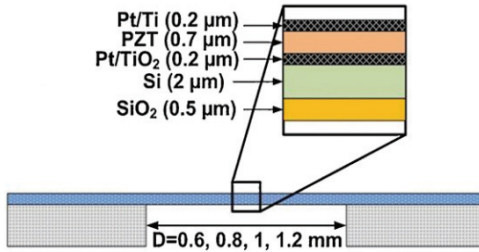


Fig. 4. Cross-section schematic of diaphragm [9].

In micro/nano scale there are many phenomena effect damping of structure that are negligible in macro scale. Some of these phenomena have some other effects that have major impact on vibrational behavior of the structure. For example, squeeze film has effects on both damping and mechanical stiffness of the structure. However, the total effect of damping in structure is estimated by a quantity called quality-factor, the effect of quality-factor is obvious from vibration basic equation below [12],

$$\ddot{x}(t) + \frac{\omega_n}{Q} \dot{x}(t) + \omega_n^2 x(t) = \frac{f(t)}{m_{eff}}. \quad (25)$$

The quality-factor in air is measured to be 137. So the value of ζ in this configuration will be 0.004.

Fig. 5 shows the comparison between experimental and theoretical values of first four natural frequencies. We can readily see that formulation of vibrational behavior in damped condition is more accurate than un-damped condition.

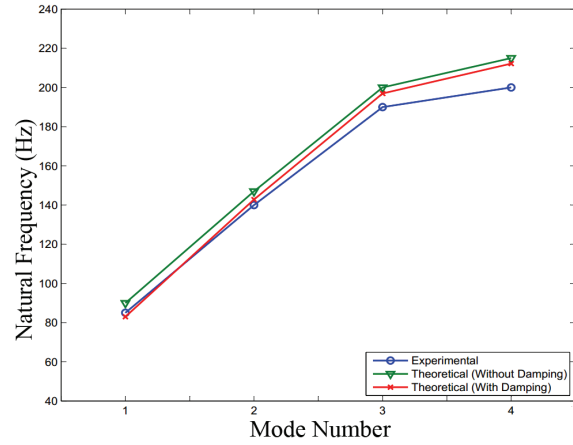


Fig 5. First four Natural Frequencies: Comparison between experimental and theoretical results.

4. Application

4.1. Gas Turbine Engines (GTEs)

Gas turbine engine (GTE) propulsion systems are used in many areas of human activity, and they have an excellent record in both reliability and safety. In this regard, a reliable condition monitoring system is especially important for aircraft GTEs, because a fault in the GTE can lead to disastrous results. However, real-time condition monitoring of such complex nonlinear dynamic systems is a very complicated problem. During normal operation, the GTEs experience significant changes in pressure, temperature, Mach number, and power output. These intrinsic variations will alter the GTE dynamics in a nonlinear manner. Hence, careful attention must be paid during GTE operation to ensure that the mechanical, aerodynamic, thermal, and flow limitations of the GTEs are maintained [1].

4.2. Dynamic Pressure Measurement

In-situ dynamic pressure measurements have a very good potential to provide GTE diagnostics, maintenance management, and optimized performance, based on pressure variation measurements. The versatility of pressure-based measurements will provide a foundation for active-control methodologies through the evaluation and interpretation of changes to the dynamic pressure flow within the GTE environment.

Application of traditional bulky and off-line pressure sensors does not provide very useful

condition monitoring of GTEs. So a new approach introduced by Rinaldi et al. is to use MEMS based dynamic pressure sensor for condition monitoring of GTEs. In the work done by Rinaldi et al., application of MEMS based dynamic pressure sensor on J-85 engine have been studied (shown in Fig. 6 and 7) [1].



Fig. 6. J-85 engine [1].



Fig 7. J-85 engine cutaway [1].

Dynamic pressure, by definition, consists of a variation in pressure over a given time interval. This is especially true for rotating machinery such as fans, where the dynamic pressure flow is generated by the rotation of the fan blades. In this regard, for the work presented here in, the time dependence of the pressure flow is taken from the point of view of the individual GTE fan blades passing beneath a reference point (sensor location) as shown in Fig. 8. With this implementation some parameters could be monitored: (1) the speed of the rotary fans, (2) the health of single blades, and (3) radial and axial alignment of fans.

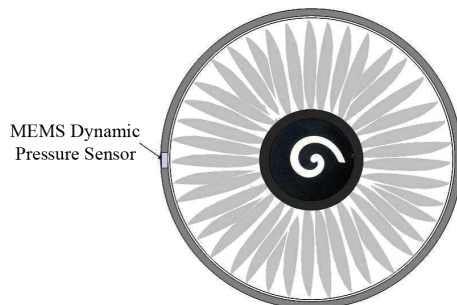


Fig. 8. Schematic front-view of the location of the MEMS dynamic pressure sensor with respect to the fan blades of a GTE [1].

4.3. MEMS Pressure Sensor Specifications

Due to their low-pressure sensitivity, MEMS silicon microphones are proposed as the main components of the sensor for monitoring the dynamic pressure variations generated by the GTE fan and compressor stages. The sensor consists of two Knowles Acoustics SiSonic microphones. Two microphones were used for redundancy in the measurements. This is an added advantage in using small scale components as they allow for redundancy even within a small surface area and provide added system reliability. Presented in Fig. 9 is an image of the main component of the MEMS microphone. The active area of the silicon diaphragm has a diameter of 500 μm and a thickness of 1 μm [1].

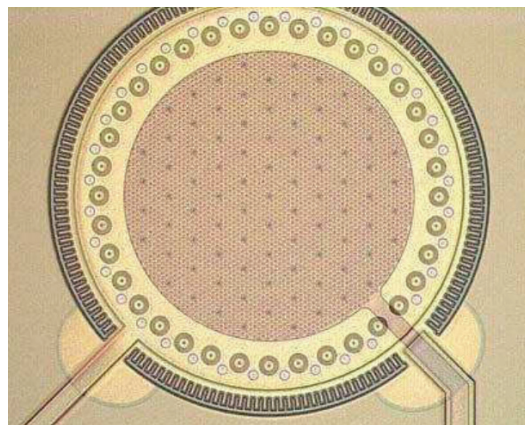


Fig 9. MEMS SiSonic microphone diaphragm [1].

With the specifications above we can use equation (14) to determine natural frequencies of pressure sensor. With the assumption of no internal tension and discarding damping effects, the first and second natural frequency will be 15.6 and 32.5 kHz, respectively.

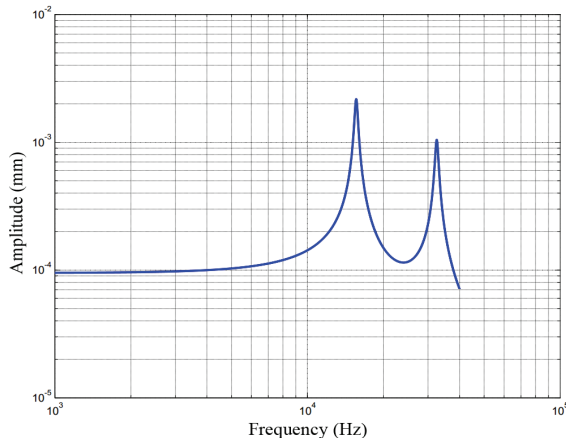
4.4. Gas Turbine Engine Tests

As we said, J-85 engine have been used for this illustration. The J-85 engine has 8 compressor stages on a single shaft. Given in Table 1 is the number of blades for the stages, and the theoretical nominal RPM and stage-frequency at engine idle and 80 % of maximum power. In this regard, the stage-frequency is defined as the frequency detected by the sensor for that particular stage at a given engine operating condition.

As it is obvious from Table 1, the working frequency is up to about 32 kHz. So this range of operation includes only two of first natural frequencies. These operating conditions help the sensor to reach its maximum signal output. Fig. 10 shows frequency response of pressure sensor for two, first natural frequencies [1].

Table 1. An overview of the compressor stages [1].

| Compressor Stage | Number of Blades | Nominal RPM @ 80% | Nominal Frequency (Hz) @ 80% |
|------------------|------------------|-------------------|------------------------------|
| 1 st | 30 | 13400 | 6923 |
| 2 nd | 60 | 13400 | 13400 |
| 3 rd | 87 | 13400 | 19430 |
| 4 th | 106 | 13400 | 23673 |
| 5 th | 131 | 13400 | 29257 |
| 6 th | 132 | 13400 | 29480 |
| 7 th | 140 | 13400 | 31267 |
| 8 th | 120 | 13400 | 26800 |

**Fig. 10.** Estimated frequency response of pressure sensor in J-85 engine operation range.

5. Discussion

As we saw in section 2, the theoretical model to predict vibrational behavior of circular microdiaphragms is investigated. This formulation includes damped conditions. The damping effects are mainly different in micro- and macro-scale. Energy dissipation mechanisms do not equally contribute to the total energy loss of the system. Size and ambient pressure are the two main parameters, which clarify the contribution of these terms. Size reduction from macro to micro scale increases surface-to-volume ratio, and hence signifies the effect of surface forces, and dominates them over the body forces. Therefore, bulk losses are negligible in micro-scale regions compared to medium damping terms. The main energy dissipation mechanisms are identified as (a) medium loss, which is the loss into the surrounding (fluid) medium due to acoustic radiation or viscous drag, (b) clamping or support loss, which is the dissipation of energy through the support, and (c) bulk loss, which is composed of a variety of physical mechanisms, such as internal friction, thermoelastic dissipation (TED), phonon-phonon scattering, motion of lattice defects, and piezoelectric damping in piezoelectric materials. Effect of these phenomena in damping is different so to determine the damping coefficient all conditions should be checked and their effects should be considered.

The effect of internal tension should not be neglected. The value of internal tension determines the actual behavior of microdiaphragm. Microfabrication methods often involve high temperature thin film deposition processes, and the mismatch between thermal expansion coefficients of different layers could cause internal tension.

The validation of formulation shows that introduction of damping in modeling decreased difference between theoretical and experimental results. The remained error could be for difference in properties of materials, instrument errors and skipping some phenomena that have effect on damping like squeeze film effect.

As we saw in section 4, the application of microdiaphragm based pressure sensor in dynamic pressure condition monitoring of GTEs has major impact on health management and performance improvement of these systems. As discussed before, with this implementation some parameters could be monitored: (1) the speed of the rotary fans, (2) the health of single blades, and (3) radial and axial alignment of fans. Two of first natural frequencies of proposed sensor are in the operational range of testing GTE. This could help for better performance of condition monitoring, because of high amplitude signal output and noise cancelation. The high sensitivity associated with acoustic dynamic pressure measurements allowed for the extraction of pressure signals J-85 engine.

6. Conclusions

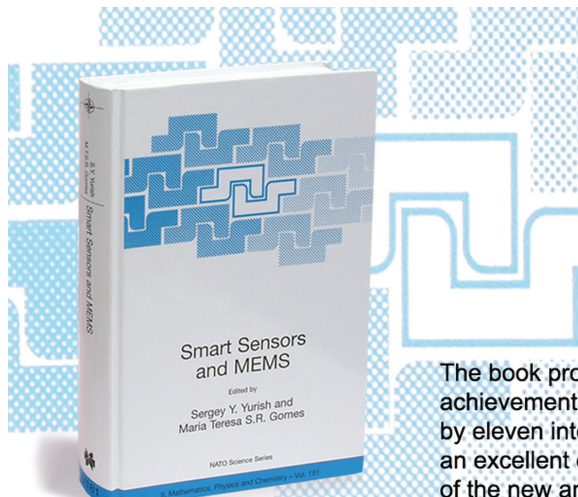
In this paper, we investigated vibrational behavior of piezoelectric microdiaphragm based pressure sensor with application for GTEs condition monitoring. The general formulation based on transverse vibration of circular plates introduced and the response of diaphragm under forced excitation has discussed. The validation of theoretical models with experimental results shows that introduction of damping effect in theoretical modeling improves the vibrational behavior prediction. Application of MEMS pressure sensors for condition monitoring of GTEs offers special features. In-situ dynamic pressure measurements have a very good potential to provide GTE diagnostics, maintenance management, and optimized performance, based on pressure variation measurements.

References

- [1]. G. Rinaldi, I. Stiharu, M. Packirisamy, V. Nerguzian, R. J. Landry, J. P. Raskin, Dynamic pressure as a measure of gas turbine engine (GTE) performance, *Measurement Science and Technology*, Vol. 21, No. 4, 2010, 045201.
- [2]. K. T. Kim, J. G. Lee, B. D. Quay, D. A. Santavicca, Spatially distributed flame transfer functions for predicting combustion dynamics in lean premixed gas turbine combustors, *Combustion and Flame*, Vol. 157, No. 9, 2010, pp. 1718-1730.

- [3]. V. Muralidharan, V. Sugumaran, Feature extraction using wavelets and classification through decision tree algorithm for fault diagnosis of mono-block centrifugal pump, *Measurement*, Vol. 46, 2013, pp. 353-359.
- [4]. L. Barelli, G. Bidini, F. Bonucci, Diagnosis methodology for the turbocharger groups installed on a 1MW internal combustion engine, *Applied Energy*, Vol. 86, No. 12, 2009, pp. 2721-2730.
- [5]. J. M. Luján, V. Bermúdez, C. Guardiola, A. Abbad, A methodology for combustion detection in diesel engines through in-cylinder pressure derivative signal, *Mechanical Systems and Signal Processing*, Vol. 24, No. 7, 2010, pp. 2261-2275.
- [6]. S. Fricke, A. Friedberger, H. Seidel, U. Schmid, A robust pressure sensor for harsh environmental applications, *Sensors and Actuators A: Physical*, Vol. 184, 2012, pp. 16-21.
- [7]. L. Barelli, G. Bidini, C. Buratti, R. Mariani, Diagnosis of internal combustion engine through vibration and acoustic pressure non-intrusive measurements, *Applied Thermal Engineering*, Vol. 29, No. 8, 2009, pp. 1707-1713.
- [8]. M. Olfatnia, T. Xu, J. M. Miao, L. S. Ong, X. M. Jing, L. Norford, Piezoelectric circular microdiaphragm based pressure sensors, *Sensors and Actuators A: Physical*, Vol. 163, No. 1, 2010, pp. 32-36.
- [9]. M. Olfatnia, T. Xu, L. S. Ong, J. M. Miao, Z. H. Wang, Investigation of residual stress and its effects on the vibrational characteristics of piezoelectric-based multilayered microdiaphragms, *Journal of Micromechanics and Microengineering*, Vol. 20, No. 1, 2010, 015007.
- [10]. M. Olfatnia, V. R. Singh, T. Xu, J. M. Miao, L. S. Ong, Analysis of the vibration modes of piezoelectric circular microdiaphragms, *Journal of Micromechanics and Microengineering*, Vol. 20, No. 8, 2010, 085013.
- [11]. M. Sheplak, J. Dugundji, Large deflections of clamped circular plates under initial tension and transitions to membrane behavior, *Journal of Applied Mechanics*, Vol. 65, No. 1, 1998, pp. 107-115.
- [12]. M. Olfatnia, Z. Shen, J. M. Miao, L. S. Ong, T. Xu, M. Ebrahimi, Medium damping influences on the resonant frequency and quality factor of piezoelectric circular microdiaphragm sensors, *Journal of Micromechanics and Microengineering*, Vol. 21, No. 4, 2011, 045002.
- [13]. M. Yu, B. Balachandran, Sensor diaphragm under initial tension: linear analysis, *Experimental Mechanics*, Vol. 45, No. 2, 2005, pp. 123-129.
- [14]. S. P. Timoshenko, S. Woinowsky-Kringer, Theory of plates and shells, New York: McGraw-Hill, 1959.
- [15]. M. Yu, X. Long, B. Balachandran, Sensor diaphragm under initial tension: nonlinear responses and design implications, *Journal of Sound and Vibration*, Vol. 312, No. 1, 2008, pp. 39-54.

2013 Copyright ©, International Frequency Sensor Association (IFSA). All rights reserved.
[\(<http://www.sensorsportal.com>\)](http://www.sensorsportal.com)



Smart Sensors and MEMS

Edited by

Sergey Y. Yurish and
Maria Teresa S.R. Gomes

The book provides an unique collection of contributions on latest achievements in sensors area and technologies that have made by eleven internationally recognized leading experts ...and gives an excellent opportunity to provide a systematic, in-depth treatment of the new and rapidly developing field of smart sensors and MEMS.

The volume is an excellent guide for practicing engineers, researchers and students interested in this crucial aspect of actual smart sensor design.

Order online: www.sensorsportal.com/HTML/BOOKSTORE/Smart_Sensors_and_MEMS.htm